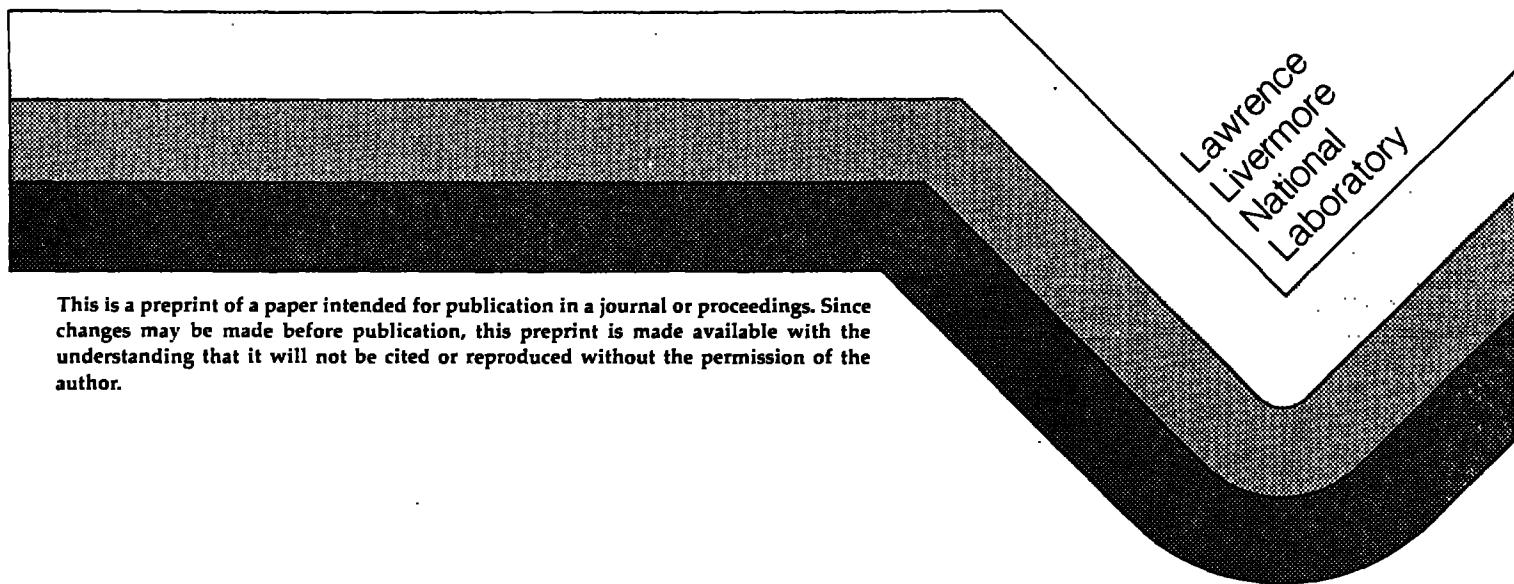# SHOCK TEMPERATURES AND MELTING IN CsI

H. B. Radousky, M. Ross, A. C. Mitchell and W. J. Nellis

University of California, Lawrence Livermore National Laboratory

Livermore, California 94550

SHOCK TEMPERATURES AND MELTING IN CsI*

H. B. Radousky, M. Ross, A. C. Mitchell and W. J. Nellis
University of California, Lawrence Livermore National Laboratory
Livermore, California 94550

ABSTRACT

Shock temperature measurements have been made on CsI up to 10,800 K and 0.9 Mbar. Melting has been observed to occur at 0.25 Mbars and 3500 K. A simple model for melting based on the packing of soft spheres is shown to adequately describe the data. The results suggest that in the liquid along the freezing line, there is a gradual pressure-induced change from an open NaCl-like structure to one in which atoms are arranged as in a close-packed monatomic fluid. Above 5000K, electronic excitation is observed to occur due to the high shock temperatures generated and the narrowing of the CsI band gap under pressure.

I. Introduction

CsI is an ideal material with which to study both insulator to metal transitions (IMT) and melting under high pressure. The interest in CsI is due in part to the fact that it is isoelectronic to the rare gas solid Xe, which has been the center of attention for metallization studies.[1-4] Both substances consist of atoms with filled $(5p)^6$ shells separated by a large energy gap from an empty conduction band and are believed to become metallic as the result of band closure.[5,6] A number of both static and dynamic high pressue studies of CsI have been performed. These include x-ray[8-12] and optical absorption measurements[11,12] in a diamond anvil cell (DAC), Hugoniot measurements[13,14] and electrical conductivity[15] behind the shock front. Under high pressure the band gap of these insulators will begin to shift, until at sufficient pressure the 5d band of cesium and the 4p band of iodine will overlap, and metallization will occur.[5] The metallization pressure of CsI[5,6] ($\sim$1 Mbar) is predicted to be lower than Xe ($\sim$1.3 Mbar) which is physically sensible since CsI starts with a band gap at zero pressure of 6.4 eV, while Xe has a zero pressure gap of 9.3eV. Using Herzfeld's criteria[1,7] also places the IMT of CsI near 1 Mbar.

Shock wave studies can play a valuable role in the study of the IMT, as in the case of Xe.[2] Shock waves can generate the required Mbar pressures and densities necessary to study band closure in these materials. In addition, the high shock temperatures generated, on the order of thousands of degrees K, cause significant numbers of electrons to be excited over the rapidly closing gap. Temperature measurements in this region are extremely useful, in that they allow us to study the partition of energy between internal energy and electronic excitation. Coupled with theory, these measurements can be used to test various models for the band closure in these materials.

Temperature measurements also allow us to study phase transitions under shock conditions. Shock transitions such as melting, which can be barely descernible in a pressure-volume plane, show up quite dramatically in the

pressure-temperature plane. This was first demonstrated in the pioneering work on alkali-halides by Kormer.[16,17] CsI, whose shock melting transition has never been studied, is especially appropriate, again due to its similarity to Xe.

In this paper we report the first shock temperature measurements on CsI, with measurements performed from 240 to 930 kbars, and corresponding temperatures of 3,500 to 10,800 K (1 eV = 11,600 k). Sections II and III describe the experimental details and analysis, Section IV presents a theoretical treatment of the data, while Section V presents a discussion of the results.

II. Experimental Procedures

The shock temperatures of CsI were measured using a six channel optical pyrometer and were performed on the LLNL two-stage light-gas gun.[18] The gun can accelerate a flat projectile up to 8 km/sec, which is then impacted on the sample to generate a planar shock wave in the material. In this case an aluminum impactor was used to generate a shockwave in the CsI sample. A diagram of the experimental configuration is shown in Figure 1a. The impactor velocity u_I was measured using a flash x-radiograph system. The resulting shock pressue in CsI was calculated using u_I, the method of shock impedance matching,[19] and the Hugoniots of both CsI and the aluminum impactor.

When the planar shock moves through the CsI sample, the material is compressed and irreversibly heated to thousands of degrees. The shock represents a sharp discontinuity moving through the sample, such that the material behind the front is compressed and very hot, while ahead of the front, the sample is still at ambient pressure and temperature. The hot material behind the shock front is sufficiently opaque to emit thermal radiation in the visible region of the spectrum. This radiation can escape in the forward direction through the unshocked and still transparent material. The technique is based on observing thermal radiation emitted from electrons behind the shock front which are in thermodynamic equilibrium with the lattice. This is a reasonable assumption, since electron-phonon interaction times are on the order of 10^{-14} sec, while the measurement has a time scale of 10^{-8} sec.

The pyrometer, which has been described in detail previously,[20] consists of silicon photodiodes which measure the light intensity emitted from the shock heated sample at six different wavelengths ranging from 450-800 nm. For temperatures below 6000 K, the uncertainties in T are ± 200 K and in ε they are ± 0.15. At the higher temperatures, the sensitivity of the pyrometer decreases, which results in uncertainties of ± 500 K. This change in sensitivity is due to the movement of the blackbody peak toward the ultraviolet with increasing temperature. Since we are using a pyrometer which looks at visible light, it is most sensitive at temperatures below 6000 K. The output of the photodiodes is recorded using fast oscilloscopes and film. Two trigger pins are placed next to the sample. When the CsI is shocked, the pins send out a pulse which triggers the oscilloscope sweep.

An oscillogram from the 450 nm channel of our pyrometer is shown in Figure 1b. The record was from shot CsI 7 (T = 8800 K). The signal rises as the shock enters the CsI, and plateaus as the shock traverses the material. The plateau indicates that a steady shock wave is present in the sample and persists until the shock reaches the rear surface, where the pressure is released. The magnitude of the voltage signals is related to the actual light intensity emitted from the CsI through a calibration of the system against a tungsten ribbon lamp, whose spectral radiance is known.

The CsI samples were single crystals of good optical quality, which were obtained from Janos optical. Care was taken not to expose the sample to moisture, since CsI is very hygroscopic. Optical absorption measurements were performed for CsI on a Cary 17 spectrometer. The absorption was nearly wavelength independent, with the absorption changing from 22% to 17% over the 450-800 nm range. This sample absorption was included in the system calibration along with losses at the turning mirror.

Temperatures along the CsI Hugoniot were measured at seven pressures from 240 to 920 kbars, with the change in pressure resulting from a change in impact velocity.

III. Data Analysis and Results

The data for the seven sets of measurements are shown in Fig. 2. The temperature was determined by least square fitting the data to a Planck greybody spectrum,

$$N(\lambda) = \frac{\epsilon C_1}{\lambda^5} [e^{C_2/\lambda T} - 1]^{-1} \tag{1}$$

where $N(\lambda)$ is the spectral radiance, λ is the wavelength, $C_1 = 1.19 \times 10^{16} W\text{-}m^2/sr$, $C_2 = 1.44 \times 10^{-12} m\text{-}K$ and ϵ is a wavelength independent emissivity. The least square fits to the data are shown in Fig. 2.

The results, plotted as temperature versus volume, are shown in Fig. 3 and tabulated in Table I along with other relevant parameters. The data above 4000 K appears to fall on a straight line. $(dT/dV)_{Hugoniot}$ was found to be 1466 $(\frac{K\text{-}mole}{cm^3})$. The maximum pressure of 922 kbars corresponds to a volume of 27.2 cm^3/mole, which is still somewhat larger than the Herzfeld prediction for metallization of CsI at 24.4 cm^3/mole. To reach the Herzfeld volume in CsI would require a shock pressure of approximately 1.6 Mbars, which would result in temperatures which are beyond the range of our present visible pyrometry system. At a volume of 27.2 cm^3/mole, the optical data of Asaumi et al.,[11] indicate a band gap of approximately 1 eV. Since the corresponding shock temperature is also nearly 1 eV (11,600 K = 1 eV), we expect a significant amount of electronic excitation over the gap. This point is discussed more fully in Sections IV and V.

Below 4000K, the data shows an abrupt change in slope, which can be attributed to the melting transition. Similar results have been obtained by Kormer[16,17] for other alkali halides. Also shown in Fig. 3 are the theoretical results due to Aidun, et al.[6] for solid CsI. These calculations were made using finite strain theory in which the crystal energy is expressed as a polynomial and thermal properties are calculated in the harmonic approximation using Grüneisen theory. Below the melting transition, the

theory appears to do very well, while above 4000 K, the necessity of accounting for the melting transition is clear. A theory for CsI, which takes into account the liquid and solid phases as well as electronic excitation is described in the following section.

An estimate for the heat capacity, C_v of CsI can be made from the measured P-V and T-V data along the Hugoniot. Using a Grüneisen model, Keeler and Royce[21] obtained the result

$$C_v = \frac{(\partial E/\partial V)_H + P}{(\partial T/\partial V)_H + (\frac{\gamma}{V})T}$$

(2)

where P, V, E and T are the Hugoniot pressure, volume, internal energy and temperature. The partial derivatives are taken along the Hugoniot, and γ is the Grüneisen parameter. While $\gamma(V)$ is not known experimentally for CsI, we can obtain a lower bound for C_v by taking $\gamma = 0$. The heat capacities obtained are plotted in Fig. 4. C_v below 3000 is shown as 3R which is the high temperature limit for an harmonic solid. At 3500 K, a sharp peak in C_v is observed due to melting. This peak comes from the $(\partial T/\partial V)_H$ term in (2), which shows a corresponding sharp change in slope at this temperature, while the terms in the numerator are smoothly varying. The broad maximum above 5000 K is understood qualitatively as due to the electronic excitation. That is, as electrons are thermally excited with increasing temperature, C_v increases from the lattice value. At higher shock temperatures and densities the energy gap decreases and causes C_v to decrease.

IV. Theoretical Calculations

Accurate Hugoniot calculations for high density-high temperature salts are severely hampered by a lack of knowledge of the intermolecular forces and in the case of CsI by complications arising from thermal electronic excitation and possible metallization. Therefore, as a first approximation, we employ a computationally simple model for CsI that takes advantage of its similarity with Xe.

The similarity in the equation of state of Xe and CsI is reflected by the agreement of the high pressure isotherm between two sets of augmented-plane-wave (APW) calculations both made with local density Hedin-Lundquist exchange and correlation energy (Fig. 5). Although the calculations for Xe were made for an fcc lattice, and in CsI atoms are in the bcc packing, the P-V curves for these two structures are known to differ only slightly. The agreement between the Xe and CsI calculations suggests that that at high pressure, it is the repulsive forces that dominate the thermodynamic properties and that the very slowly varying Coulomb potential of CsI represents a minor contribution to the pressure. For example at the room temperature equilibrium density of the solid the contribution of the ionic charges to the total pressure amount to -21.6 kbar. But at 560 kbar, this contribution increases to -56.4 kbar and is only 10%. This of course is not the case for the total energy where Coulomb terms make a very large contribution to the cohesive energy. But this is not important since we will only be interested in energy differences. The increasing contribution to the pressure by the repulsive forces at high temperature will improve this approximation.

We assume the properties of CsI can be determined by treating each ion as being xenon-like, in which the influence of the long range coulomb force is absorbed into the parameters of an "averaged ion" exponential-six (exp-6) potential

$$\phi(r) = \frac{\varepsilon}{k} \left[\left(\frac{6}{\alpha-6}\right) \exp \left(\alpha(1 - \frac{r}{r^*})\right) - \left(\frac{\alpha}{\alpha-6}\right)\left(\frac{r^*}{r}\right)^6 \right] \tag{3}$$

The parameters chosen to best fit the higher pressure portion of the CsI isotherm are $\alpha = 13.0$, $\varepsilon/k = 235$ K and $r^* = 4.40$Å. These differ from the values previously used for shock compressed Xe only in r^* which for Xe is 4.47Å. But omitting the Coulomb term makes it difficult (if not impossible) to fit both the high and low pressure part of the isotherm. As a result the calculated pressure for CsI at the 300 K equilibrium density is 13.9 kbar. The calculated 0 K isotherm is shown as the dashed line in Fig. 5. However, this pressure which is appreciably in error at the start of a Hugoniot calculation makes only a small contribution to the final pressure and is well within experimental uncertainty. The Hugoniot is calculated by satisfying the relationship[22]

$$E - E_0 = \frac{1}{2} (P + P_0)(V_0 - V) , \tag{4}$$

where E, P, V are respectively, the total energy, pressure and volume and the subscripted variables denote their initial values. Although the exp-6 potential does not calculate E_0 correctly, only the energy difference ($E - E_0$) appears in the Hugoniot relation (Eq. 4).

Following the procedure of earlier work, Hugoniot calculations were made using the Lennard-Jones-Devonshire[23] (LJD) cell model for the solid phase, soft-sphere perturbation theory[24] for the fluid and a semiconductor model to calculate the electron thermal properties.[24,25]

In the LJD model each atom is confined to a cell and moves about in the spherically averaged field of its neighbors. In the case of CsI, which has a "CsCl" structure, each atom is arranged in a bcc structure and interacts via the "averaged ion" potential [Eq. (1)]. For the case of the liquid, the use of fluid perturbation theory is equivalent to assuming that the atoms are arranged in a roughly close-packed order as in a monatomic or hard sphere liquid. This is known not to be the case for liquid CsI at atmospheric pressure, where the large volume change on melting (28.5%) as well as the x-ray and netron diffraction data have been interpreted as evidence the liquid has an open NaCl-like structure with about 6 nearest neighbors. But in the present case the liquid phase does not appear until about a 40% compression along the Hugoniot. At these high pressure conditions the repulsive forces will dominate the properties and lead to a close packed-like atomic arrangement. We demonstrate a posteriori that our use of fluid perturbation theory is valid in this regime.

The expressions for the total energy and pressure are similar to those used in calculating the Xe Hugoniot. They are

$$E(V,T) = E_n(V,T) + \Delta E(V)N_e(V,T) + E_e(V,T) \tag{5}$$

$$P(V,T) = P_n(V,T) - \frac{\partial \Delta E}{\partial V} N_e(V,T) + P_e(V,T) , \tag{6}$$

$$N_e(T,V) = 2(g_v g_c)^{1/2} \left(\frac{2\pi kT}{h^2}\right)^{3/2} \frac{V}{N} (m_v^* m_c^*)^{3/4} \exp\left[-\frac{\Delta E(V)}{2kT}\right], \qquad (7)$$

and E_n and P_n are the nuclear motion contributions to the total energy and pressure calculated using the exp-6 potential. ΔE is a volume dependent conduction band gap, m_v^* and m_c^*, the effective masses in the valence and conduction band were set to 1 and g_v and g_c, the degeneracies of the p and d-like states are 3 and 5. The intermolecular repulsions are assumed to be unaffected by electronic excitation.

V.   Discussion

Figures 6 and 7 compare Hugoniot and shock temperature measurements with calculations using three different electron models. Figure 7 also includes an estimate of the P vs. T at freezing based on the widely used observation that along this curve the hard sphere fluid packing fraction has the value $\eta = 0.45$. Curves A and B were obtained using the theoretical APW band gap of Aidun, et al.[6] made with Slater and Hedin-Lundquist exchange and correlation energy respectively. These curves are in general agreement with the Hugoniot and temperature data and in part justify the use of the present models. The present theory is much too crude to accurately model the complicated processes occurring and the major objective here has been to elucidate the qualitative nature of the physics. Calculations made omitting thermal excitation (curve C) are clearly too high and demonstrate the importance of including electronic effects.

Below 400 kbar and 5000 K electronic excitations are negligible and the kink observed in the P-T curve (Fig. 7) appears to be due to melting. When a substance melts at atmospheric pressure the added energy does not lead to a rise in temperature until the process has been completed. Under shock compression the pressure-temperature path passes through the melting curve as illustrated by the present data and calculations. This feature was first observed by Kormer[16] in his shock temperature measurements in NaCl and KCl. The present results show that for CsI the onset to melting occurs near 240 kbar and 3500 K at a compression (V/V_0) of 0.625.

The value of η = 0.45 at the freezing point is characteristic of "close-packed" monatomic liquids and the agreement of the predicted freezing line with the data was a surprising result, since as we noted, alkali halides are believed to have open, ordered "NaCl-like" structures in the liquid. For example, at the normal one atmosphere melting point of CsI we obtain a value of η = .35 which is consistent with an open structure. For xenon the value of η = .45 at the triple point is consistent with a hard sphere or close packed-liked liquid structure. These results suggest that with increasing compression, CsI liquid undergoes a continuous transition from an open ordered "NaCl-like" structure to a denser or closed packed-like structure which several of its nearest neighbors are ions of the same sign. For the case of KCl, calculations made with an argon-like potential predict a value of η = 0.42 near the 480 kbar shock melting point reported by Kormer, et al. and η = 0.31 at the KCl triple point. The melting curve in Fig. 7 is not expected to be correct at low pressure where the fluid retains an open structure. Measurements of the CsI melting curve in progress shows the initial slope to be considerably steeper than the one shown here.[26]

It is noteworthy that the ratio of the volume packing fraction of an fcc solid (.740) to that of a simple cubic (NaCl) solid (.524) is √2. Thus, if η = 0.45 in a close packed liquid we should expect a value of η = 0.32 in a NaCl-like system which is close to what is actually observed. Theoretical evidence for a structural change in compressed ionic liquids KCl was first demonstrated by Adams[27] using the hypernetted chain equation (HNC). He found that under increasing pressure the structure of the liquid gradually alters from an open, charge ordered arrangement to one more nearly resembling that of a simple non-ionic mixture. Our findings are consistent with those of Adams.[27] More recently Tallon[28] has suggested that alkali-halide liquids undergo a continuous transition from an NaCl-like to a CsCl-like structure along the freezing line.

In the following paper new HNC calculations are reported for CsI and several other alkali halides that support these arguments and demonstrate the general nature of the pressure-induced change in the structure of molten salts.

VI. Summary

Shock temperature measurements on the CsI have been made from 2,500-10,800 K and between 240-930 kbars. Melting is observed at 250 kbar and 3500 K and the data fits well into a simple theory involving the packing fraction of soft spheres. The theory of Aidun, et al. for solid CsI appears to work well, but must be replaced by a liquid theory above the melting transition. Electronic excitation above 5000 K is observed due to the high shock temperatures and the narrowing of the CsI band gap. The modified band gap versus pressure of Asaumi,[11] which would place metallization near 1 Mbar, in conjunction with a liquid theory for CsI gives a reasonable agreement to the experimental temperature data. The results also indicate that along the freezing line CsI undergoes a continuous transition to a more densely packed fluid.

ACKNOWLEDGMENTS

0814c/ks/mpd

Table 1. Shock temperatures and emissivities for CsI. The pressures and
volumes were obtained by shock impedance matching.

Shot	Impactor	u_I (km/s)	Pressure (GPa)[a]	Volume (cm^3/mole)[b]	Temperature (K)	Emissivity
CsI 8	Al	2.72	24.7	35.4	3,440	0.72
CsI 10	Al	3.08	29.6	34.2	3,690	1.00
CsI 9	Al	3.31	32.8	33.5	3,740	0.79
CsI 6	Al	3.69	37.9	32.5	4,210	0.94
CsI 3	Al	4.60	52.3	30.4	6,200	1.00
CsI 7	Al	5.54	69.4	28.7	8,800	0.75
CsI 4	Al	6.64	92.2	27.1	10,800	0.94

a 1 GPa = 10 kbar

b V_0 = 57.6 cm^3/mole

## Figure Captions

FIG. 1   a) Drawing of experimental design for CsI shock temperature
              measurements.

          B) Typical record from our six-channel optical pyrometer from shot
              C_sI 7, λ = 450 nm.

FIG.2   Spectral radiance, n, vs. wavelength λ, for shocked CsI.
          Temeprature and emissivities are determined by a least squares fit
          to the Planck distribution of Eq. 1.

FIG. 3   Temperature-volume curve for CsI. The sharp break at 3500 K is due
          to melting. Solid Hugoniot is the theory of Aidun, Bukowinski and
          Ross, which works well below melting.

FIG. 4   Lower bound calculated from Eq. 2, for the heat capacity of CsI
          along the Hugoniot.

FIG. 5   Comparison of APW calculations for CsI and Xe. The dashed line
          represents the 0 K isotherm calculated with Eq. (3).

FIG. 6   Comparison of CsI Hugoniot data with calculations using three
          different electron models (see text). Data from Ref. 29 and Ref.
          30. Note factor of two difference in the volume scale from Fig. 4.

FIG. 7   Comparison of theoretical calculations with measurements of the
          shock temperature in CsI. Curves A-C use the same electron models
   as Fig. 6 (see text).

REFERENCES

1. M Ross and A. K. McMahan, Phys. Rev. B, $\underline{21}$, 1658 (1980).

2. W. J. Nellis, M. van Thiel and A. C. Mitchell, Phys. Rev. Lett., $\underline{48}$, 816 (1982).

3. K. Syassen, Phys. Rev. B, $\underline{25}$, 6548 (1982).

4. K. Asaumi and T. Mori, Phys. Rev. Lett., $\underline{49}$, 832 (1982).

5. M. Ross and A. K. McMahan in Physics of Solids Under High Pressure, edited by J. S. Shilling and R. N. Shelton (North-Holland, New York, 1981).

6. J. Aidun and M.S.T. Bukowinski, M. Ross, Phys. Rev. B29, 2661, 1984.

7. K. F. Herzfeld, Phys. Rev. $\underline{29}$, 701 (1927).

8. P. W. Bridgman, Proc. Acad. Arts and Sci., $\underline{76}$, 1 (1945).

9. D. E. Hammand, M.S. Thesis, University of Rochester (1969).

10. Tzuen-Luh Huang and Arthur L. Ruoff, Phys. Rev. B $\underline{29}$, 1112 (1984).

11. K. Asuami, Phys. Rev. B $\underline{29}$, 1118 (1984).

12. E. Knittle and R. Jeanloz, Science $\underline{223}$, 53 (1984).

13. L. V. Al'shuler, M. M. Pavlovskii, L. V. Kuleshova and G. V. Simakov, Sov. Phys.-Solid State, $\underline{5}$, 203 (1963).

14. M. M. Pavlovskii, V. Ya Vashchenko and G. V. Simakov, Sov. Physics-Solid State $\underline{7}$, 972 (1965).

15. L. A. Gatilov and L. V. Kuleshova, Sov. Phys.-Solid State, $\underline{23}$, 1663 (1981).

16. S. B. Kormer, M. V. Sinitsyn, G. A. Kirillov and V. D. Urlin, Sov. Phys., JETP, $\underline{21}$, 689 (1965).

17. S. B. Kormer, Sov. Phys. Uspekhi, $\underline{11}$, 229 (1968).

18. A. C. Mitchell and W. J. Nellis, Rev. Sci. Instrum. $\underline{52}$, 347 (1981).

19. W. J. Nellis, in Practical High Pressure Measruements, edited by G. N. Peggs (Applied Science, London, 1983), pp. 69-89.

20. G. A. Lyzenga and T. J. Ahrens, Rev. Sci. Instrum. $\underline{50}$, 1421 (1979).

21. R. N. Keeler and E. B. Royce in Physics of High Energy Density, edited by P. Caldirola and H. Knoepfel (Academic, New York, 1971), p. 88.

22. M. H. Rice, R. G. McQueen and J. M. Walsh, Solid State Physics $\underline{6}$, 1 (1957).

23. J. E. Lennard-Jones and A. F. Devonshire, Proc. Roy. Soc. Lond. $\underline{A163}$, 53 (1957); M. Ross, Phys. Rev. $\underline{A8}$, 1466 (1973).

24. M. Ross, Phys. Rev. $\underline{171}$, 777 (1968).

25. N. W. Ashcroft and D. Stroud, Solid State Phys. $\underline{33}$, 1 (1978).

26. R. Boehler, 1984, private communication.

27. D. J. Adams, J. Chem. Soc. Faraday Trans. II $\underline{72}$, 1372 (1976).

28. J. L. Tallon, Phys. Lett. $\underline{72A}$, 150 (1979).

29. S. P. Marsh, LASL Shock Hugoniot Data, Los Alamos Scientific Laboratory, U. of Cal. 1980.

30. V. L. Altshuler, M. N. Pavloskii, I. V. Kuelshova and G. V. Simakov Sov. Phys. - solid state $\underline{5}$, 203 (1963).
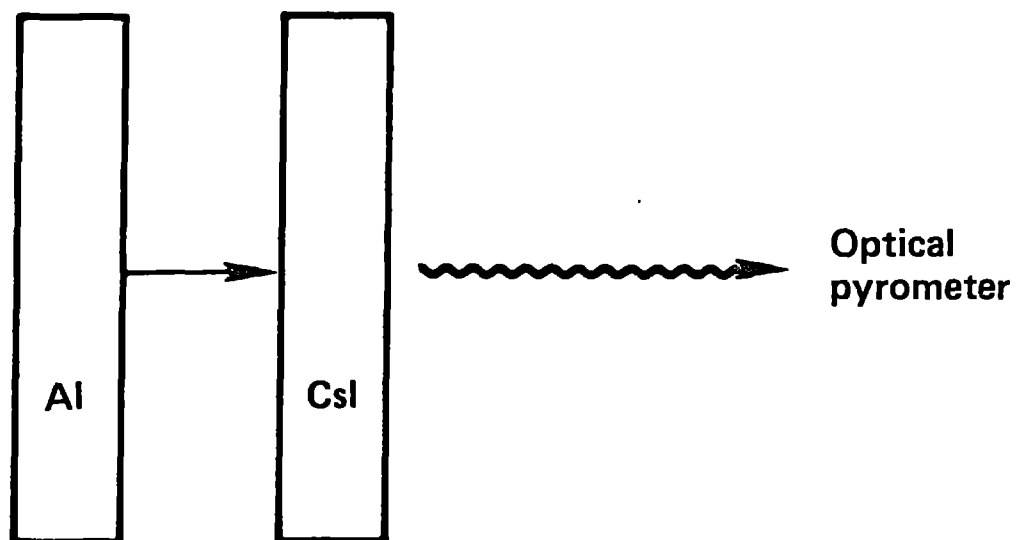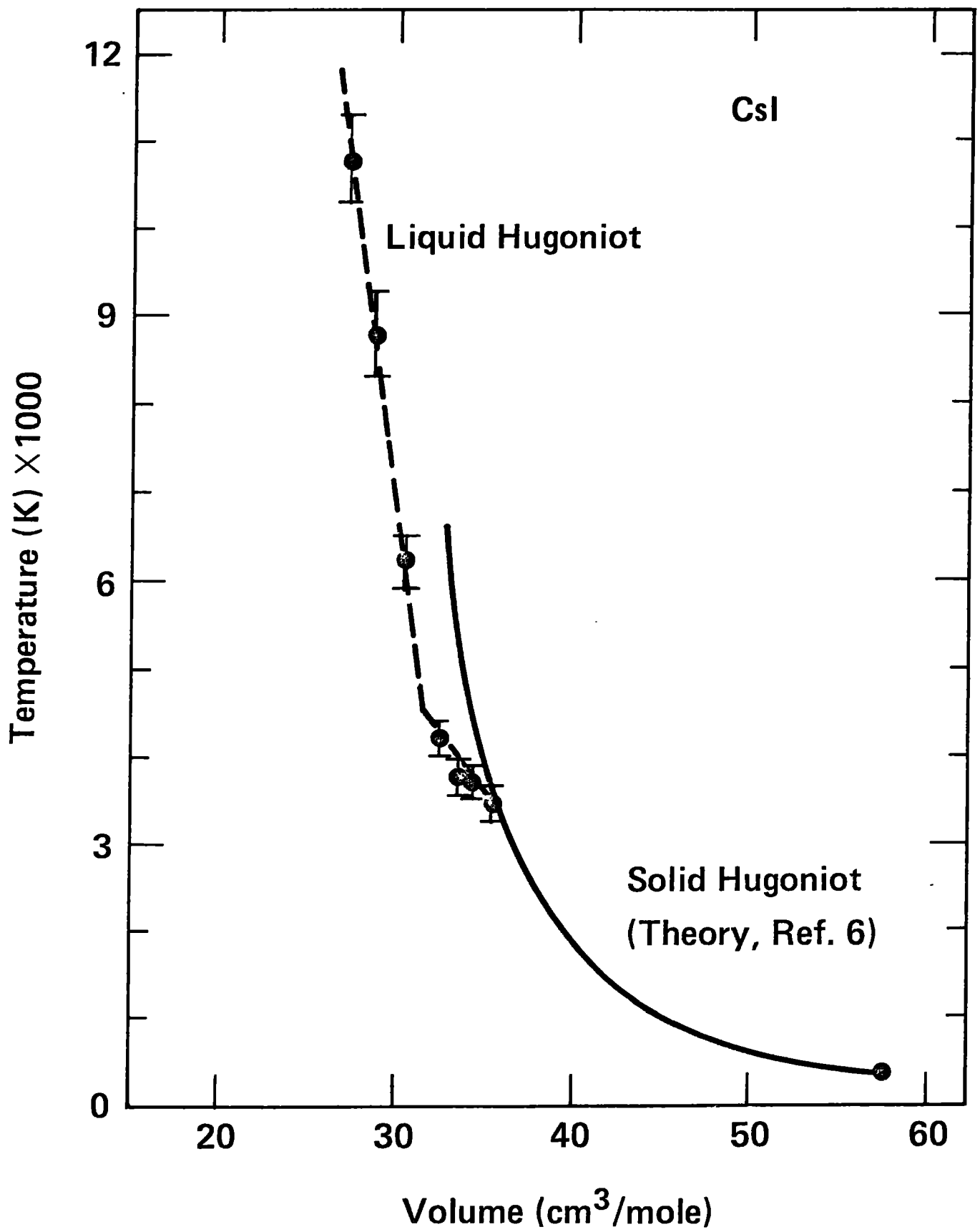
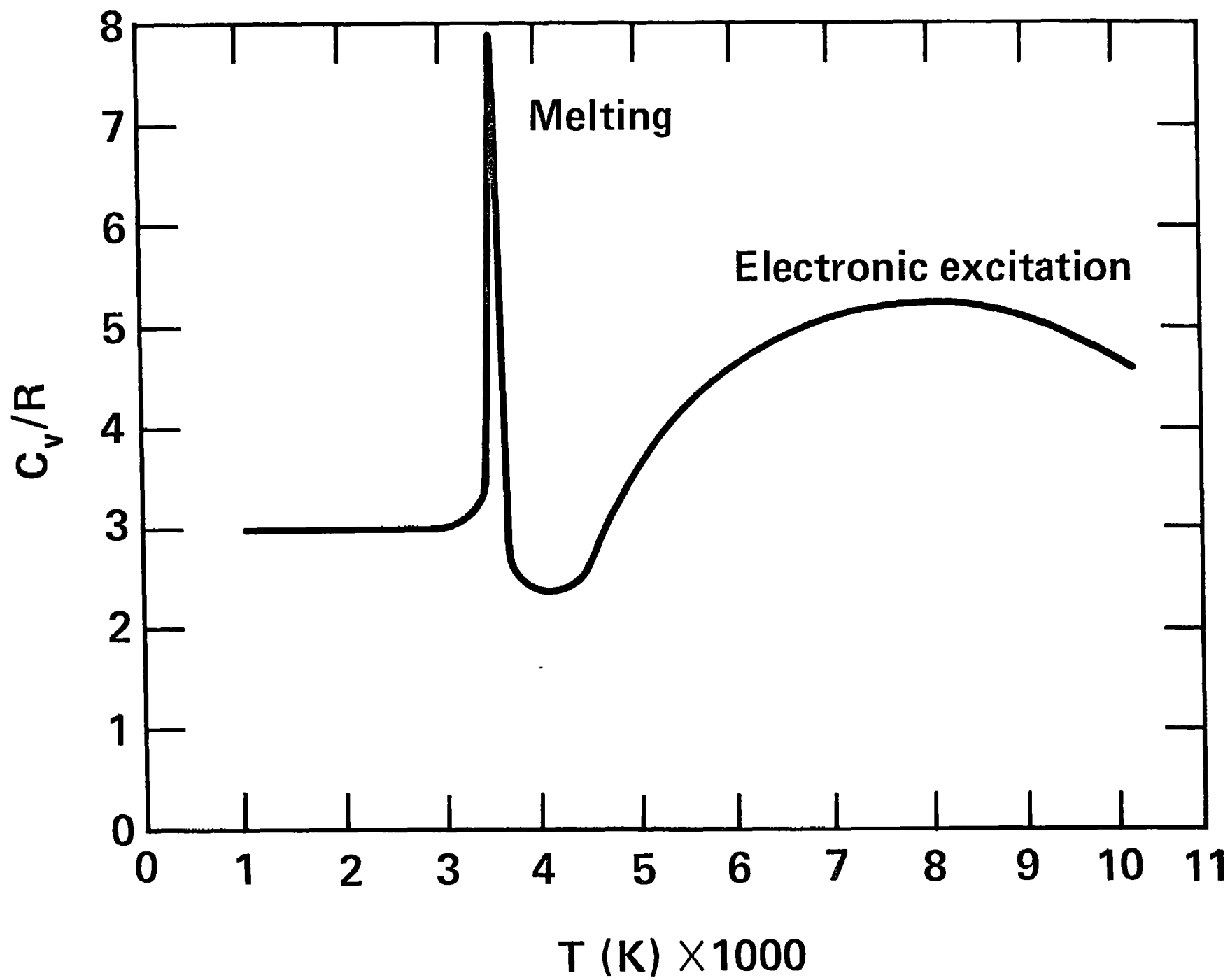(a)   Experimental configuration
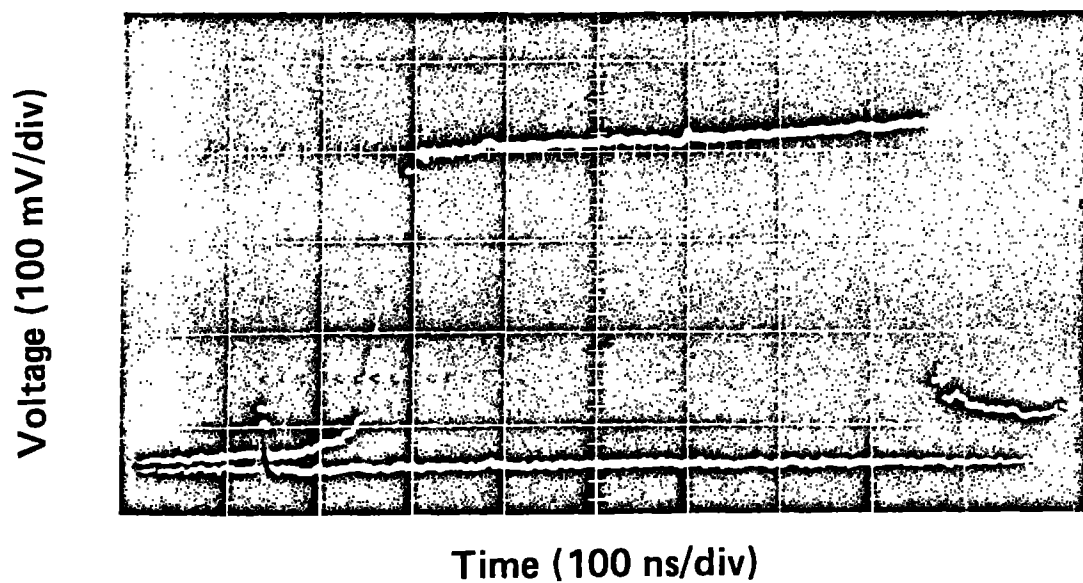
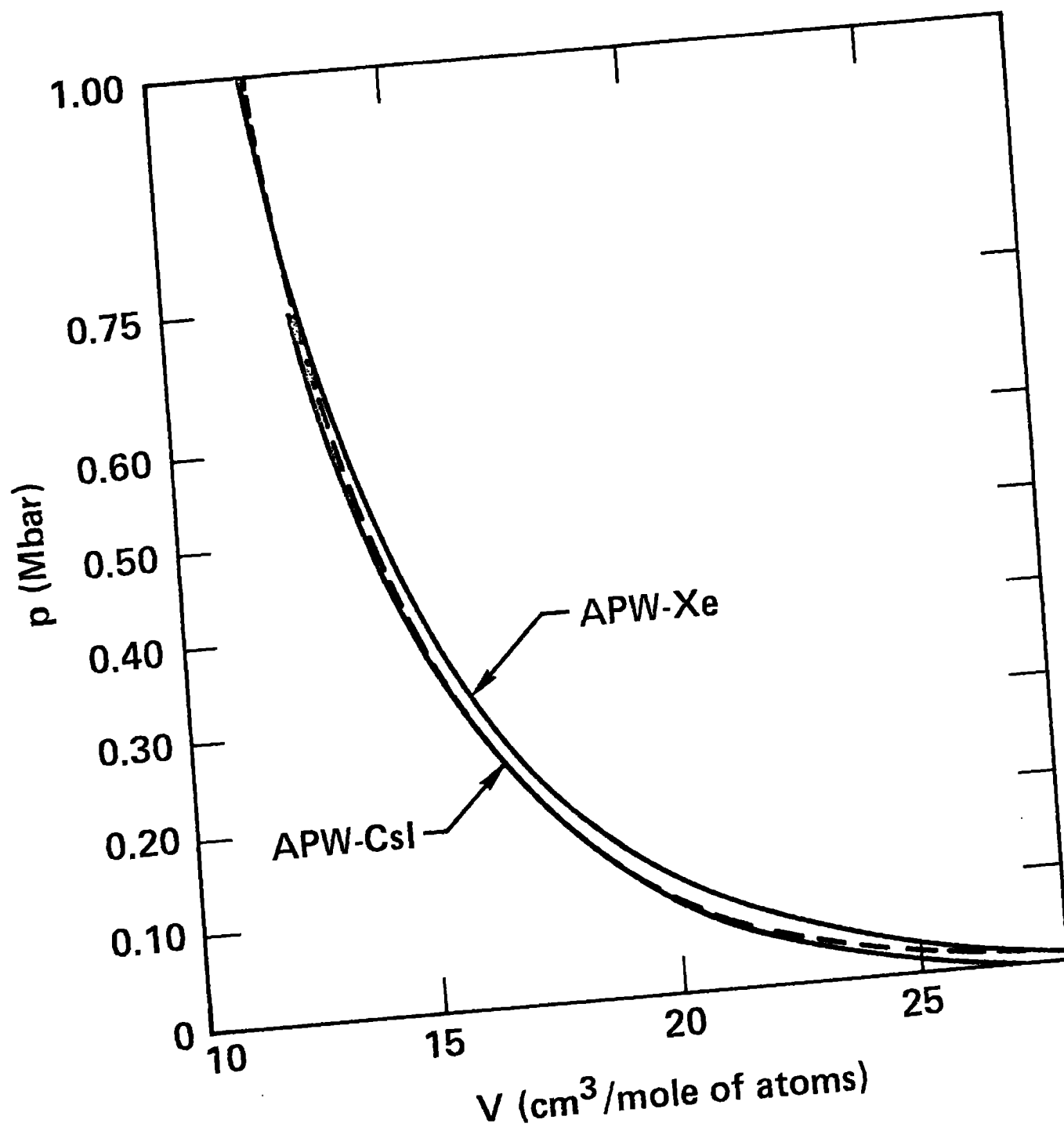(b)   Optical pyrometry record

Fig. 1
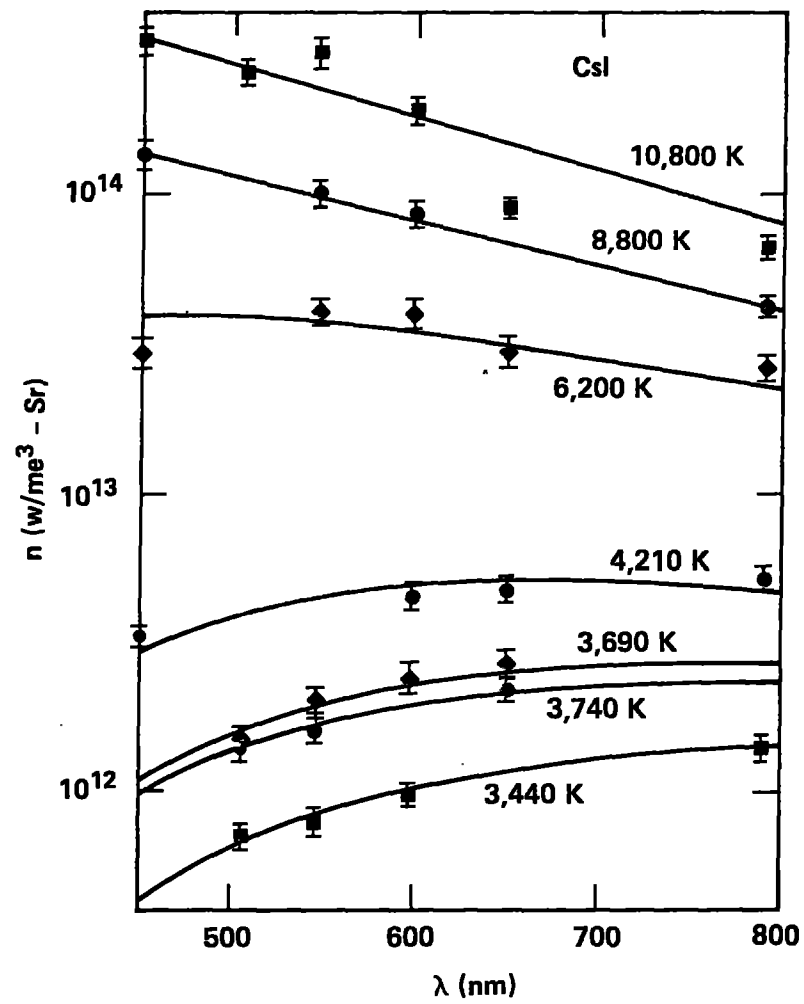
Fig. 2

Fig. 3

Fig. 4

Fig. 5

Fig. 6

Fig. 7